washed with water. A PANI precipitate was dried under at 50°C-100°C for more than 8 hours. Synthesis of PANI/PbS nano-composites The same synthesis process was adapted for preparation of PANI/PbS Nano-composite at different weight ratio of PbS nanoparticle. The PANI nanocomposite was chemically characterized by infrared spectroscopy, XRD and TGA.

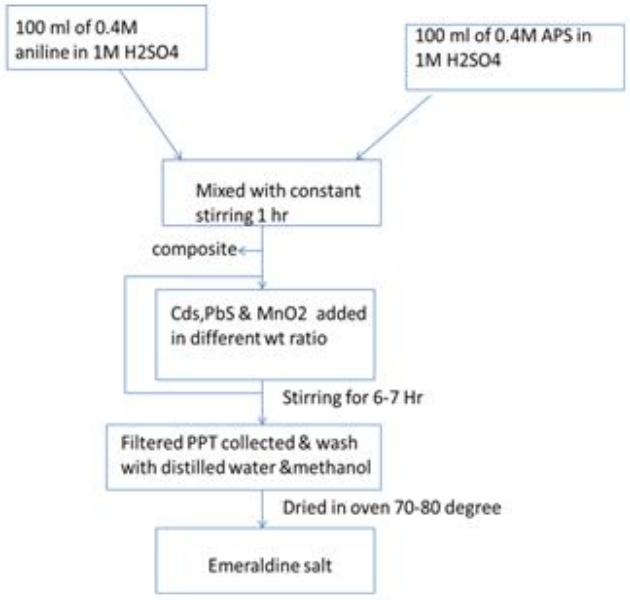

Figure 1. Chemical synthesis of polyaniline.

Characterizations of nano-composites

XRD with Philips PW-3071, using Cu-Kα radiation of wavelength 1.544 Å, with scanning rate of 20/min. at 45 KV and 40 mA. Fourier Transform Infra-Red (FTIR) spectroscopy (Model: Perkin Elmer 200) with frequency of 400 cm^{-1}-4000 cm^{-1}. Thermal analysis of sample recorded by Perkin-Elmer Diamond TGA/DTA in argon atmosphere at a heating rate of 10°C/min.

XRD characterization of pure PANI and PANI/PbS nanocoompsite: The XRD pattern of pure PANI, Pure PbS and different wt % of PANI/PbS nanocomposite are shown in the Figures 1 and 2. The particle size of crystalline particle of pure PANI and the nanocomposites are calculated by using Debye-Scherrer formula. $D=0.94\lambda/(\beta \cos\theta)$, where D is the average crystallite size (in nm), k is the shape factor which is often assigned a value of 0.94, λ is the wavelength of Cu Kα radiation (1.5418 Å), β is the full width at half maximum of the diffraction peak taking into consideration the correction due to instrumental broadening (0.09°).

Crystalline size of crystalline particle for pure PANI, Pure PbS and different wt % of PANI/PbS nano-composite are given in the Table 1 and bar graph 3.3. From the bar graph of XRD peak it is clear that as the wt % (5-20) PbS nanoparticle increases in the PANI matrix the degree of crystallites of nanocomposite also increases. Pure PANI shows crystalline reflection at specific angle in XRD pattern and amorphous at diffused background, as a result it reveals the polycrystalline structure.

SR. NO	Material	Crystalline size particle(nm)	d'spacing (Å)	2θ (°C)
1	PURE PANI	0.71	3.52	25.27
2	PURE PbS	0.95	3.21	27.77
3	5% PANI/PbS	1.048	3.23	27.56
4	10% PANI/PbS	1.42	3.24	27.47
5	15% PANI/PbS	1.23	3.012	29.65
6	20% PANI/PbS	1.437	3.009	29.68
7	25% PANI/PbS	1.438	3.0096	29.65

Table 1. Materials and crystalline size particle.

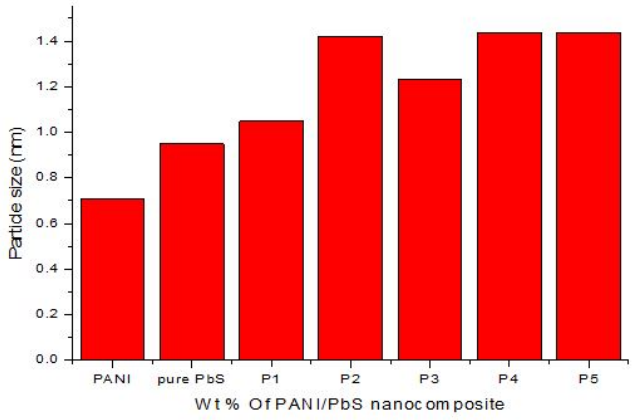

Figure 2. Crystalline size of crystalline particle for pure PANI, Pure PbS and different wt % of PANI/PbS nanocomposite.

Ultraviolet and Visible (UV-Vis) spectroscopy of PANI/PbS nanocomposite: The maximum absorption wavelength of pure PbS and PANI/PbS Nano composite are shown in the pie graph (Figures 3 and 4). In pure PbS the absorption wavelength is obtaining at 263, 277 and 768 nm. The interesting feature observed in PANI/PbS Nano composite is the presents of absorption bands at 400 to 500 nm. Because this band is not present in pure PANI as well as pure PbS this indicated that when PbS nanoparticle interacts with PANI some structural change is occurred. The presents of this band in the nano composite give the photoluminous characteristics. The polaron-π^* transition band at 320 to 385 nm becomes broader and shows the red shift. This implies that the doping state of the nanocomposites has been improved. Such phenomena can be attributed to the existence of greater number of charges on the polymer backbone by introducing nanocrystalline PbS into the polymer matrix [16].

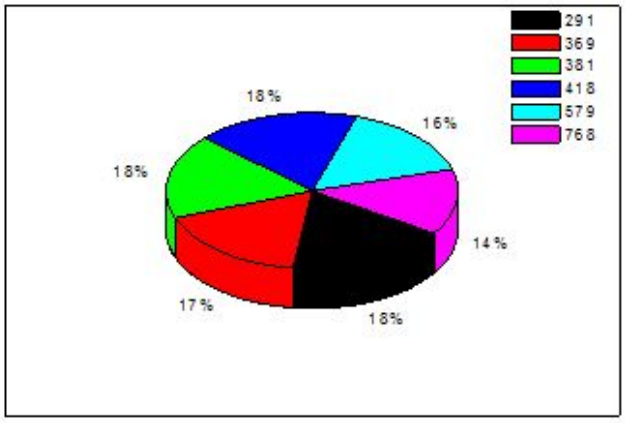

Figure 3. The maximum absorption wavelength of pure PbS and PANI/PbS nanocomposite.

Transmission electron microscopy of PANI/Pbs nanocomposite

The morphology of PANI-PbS nano composites is found out based on the TEM images. The TEM image of H_2SO_4 doped PANI is shown in Figure 4. Figures 4 and 5 depicts the TEM images of pure PbS and doped H_2SO_4 PANI/PbS.

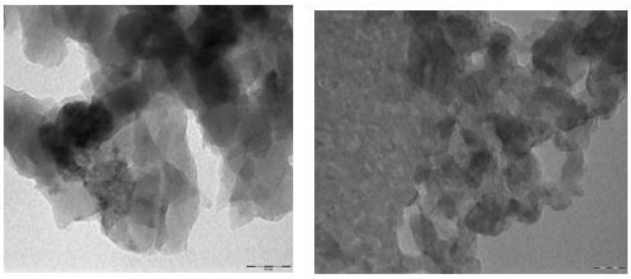

Figure 4. The TEM image of H_2SO_4 doped PANI.

TEM micrograph (10%) PANI/PbS nanocomposite shows that particles were aggregated into a big structure, although the particles were in contact with each other. Most of the particles were similar in size and have irregular rounded shapes. It is in the 100 nm scale. As the weight % PbS nanoparticle increased in the polymer than particle size decreased. The nanocomposite becomes more ordered structure, hence electrical conductivity is also increased. This is also clear by XRD and UV spectra. The average diameter of nanoparticle is 12 nm ranges.

Results and Discussion

DTA analysis of pure PANI and PANI/Pbs nano composite

Figure 5 shows DTA thermogram of PANI/PbS (5% to 25%) nanocomposite which indicated only endothermic peaks at about 230°C to 245°C due to the evaporation of water molecules trapped inside the composite or bound to the polymer backbone. whereas the change above 350°C may be assigned due to the degradation of composite. The decreased onset value of temperatures from 284°C (pure PANI) to 242.59, 244.15, 233.06, 227.55 and 237.25°C for different wt ratio of (5%-25%) PANI/PbS nanocomposite indicated that the thermal stability of nanocomposite is good than that of pure PANI which could be attributed to the retardation effect of nanostructures PbS as barriers for the degradation of PANI [15-17]. In DTA of PANI the glass transition was not observable, because the glass transition is buried in the peak due to the removal of water and it does not exhibit hysteresis. The exothermic transition observed at 99°-160°C is believed not to be Tg. Instead it would be attributed to a series of chemical reactions. The decreased peak temperatures of PANI/PbS Nano composite, further demonstrate the ordered polymer structure as well as good interfacial interactions between the metal oxide and the polymer matrix. The DSC results of composite materials are also found in good agreement with TGA results which indicates that all the nanocomposites shows minimum value of onset temperature as compare to the pure PANI. Table 2 given below gives the information of thermal parameter of Polyaniline nanocomposite with different wt percentages of PbS. Some change in the melting temperature and enthalpy in PANI/PbS (5%-25%) nanocomposite indicated miscibility with PANI matrix.

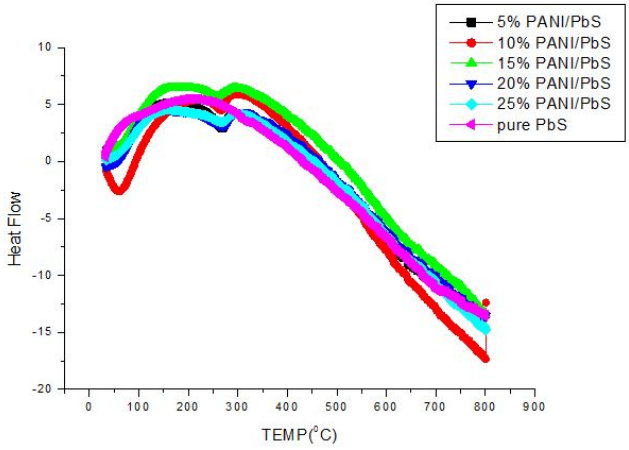

Figure 5. DTA analysis of pure PbS and PANI/PbS (5%-25%) nano composite.

Sr. No	Material	Melting temp (°C)	Onset temp (°C)	Enthalpy change (J/g)	Specific heat (Δ Cp (J/g°°C)	Peak area
1	Pure PANI	-	284	-	12.27	-
2	5% PANI/PbS	268.31	242.59	47.37	9.98	264.377
3	10% PANI/Pbs	267.88	244.15	34.46	6.52	167.613

4	15% PANI/PbS	256.81	233.06	30.4788	6.479	123.622
5	20% PANI/PbS	267.13	227.55	60.699	16.192	308.7
6	25% PANI/PbS	266.42	237.25	36.8611	9.405	152.234

Table 2. Thermal parameter of pure PANI and PANI/PbS Nano composite.

Conclusion

DTA thermal analysis indicated that the polyaniline powder had discernible moisture content. This phenomenon was in agreement with the TGA results. Moreover, in the first run of DTA thermal analysis, an exothermic peak at 150ºC-310ºC was found. This peak was due to the chain cross linking, resulting from a coupling of two neighboring -N=Q=N- groups to give two -NH-B-NH groups through a link of the N with its neighboring Quindío ring. Thus, on the basis of thermal profile of these materials, we can say that among all composite material, the Polyaniline/CdS and PANI/PbS composite materials, cross-linking or oxidative reaction starts at higher temperature than PANI/MnO_2 composites, which indicates that the thermal stability of PANI/CdS and PANI/PbS nanocomposites is higher than oxides Nano composites. These DTA results of composite materials are also found in good agreement with TGA results.

References

1. Maziarz, E Peter, Sarah A Lorenz, Thomas P White, and Troy D Wood, et al. "Polyaniline: a conductive polymer coating for durable nanospray emitters." *J Am Soc Mass Spectrom* 11 (2000): 659-663.
2. Tiitu, Mari, Anja Talo, Olof Forsen, and Olli Ikkala. "Aminic epoxy resin hardeners as reactive solvents for conjugated polymers: polyaniline base/ epoxy composites for anticorrosion coatings." *Polymer* 46 (2005): 6855-6861.
3. Ismail, Yahya A, Su Ryon Shin, Kwang Min Shin, and Seong Gil Yoon, et al. "Electrochemical actuation in chitosan/polyaniline microfibers forartificial muscles fabricated using an *in situ* polymerization." *Sens Actuators B Che* 129 (2008): 834-840.
4. Dhand, Chetna, Maumita Das, Gajjala Sumana, and Avanish Kumar Srivastava, et al. "Preparation, characterization and application of polyaniline nanospheres to biosensing." *Nanoscale* 2 (2010): 747-754.
5. Saxena, Vibha, and BD Malhotra. "Prospects of conducting polymers in molecular electronics." *Curr Appl Phys* 3 (2003): 293-305.
6. Yang, Y, and AJ Heeger. "Polyaniline as a transparent electrode for polymer light-emitting diodes: Lower operating voltage and higher efficiency." *Appl Phys Lett* 64 (1994): 1245-1247.
7. Pinto, NJ, AT Johnson Jr, AG MacDiarmid, and CH Mueller, et al. "Electrospun polyaniline/polyethylene oxide nano fiber field-effect transistor." *Appl Phys Lett* 83 (2003): 4244-4246.
8. Tan, Shuxin, Jin Zhai, Bofei Xue, and Meixiang Wan, et al. "Property in luence of polyanilines on photovoltaic behaviors of dye-sensitized solar cells." *Langmuir* 20 (2004): 2934-2937.
9. Hosseini, Seyyed Hossein, Oskouei Sh Abdi, and Ali Akbar Entezami. "Toxic gas and vapor detection by polyaniline gas sensors." *Iran Polym J* 14 (2005): 333-344.
10. Matsunaga, Tsutomu, Hideharu Daifuku, Tadashi Nakajima, and Takahiro Kawagoe, et al. "Development of polyaniline–lithium secondary battery." *Polym Adv Technol* 1 (1990): 33-39.
11. Wang, Hualan, Qingli Hao, Xujie Yang and Lude Lu, et al. "Graphene oxide doped polyaniline for supercapacitors." *Electrochem Commun* 11 (2009): 1158-1161.
12. Kovalenko, Igor, David G. Bucknall, and Gleb Yushin. "Detonation nanodiamond and onion-like-carbon-embedded polyaniline for supercapacitors." *Adv Funct Mater* 20 (2010): 3979-3986.
13. Blaz, Edyta, and Jan Pielichowski. "Polymer–Supported Cobalt (II) catalysts for the oxidation of alkenes." *Molecules* 11 (2006): 115-120.
14. Huang, Xiubing, Ge Wang, Mu Yang and Wanchun Guo, et al. "Synthesis of polyaniline-modified Fe3O4/SiO2/TiO2 composite microspheres and their photocatalytic application." *Mater Lett* 65 (2011): 2887-2890.
15. Heera, TR, and L Cindrella. "PbS/CoS–Pani composite semiconductor films." *Mater Sci Semicond Process* 14 (2011): 151-156.
16. Li, Qiaoling, Cunrui Zhang, and Jianqiang Li. "Photocatalysis and wave-absorbing properties of polyaniline/TiO_2 microbelts composite by *in situ* polymerization method." *Appl Surf Sci* 257 (2010): 944-948.
17. Wang, Ying, and Norman Herron. "Semiconductor nanocrystals in carrier-transporting polymers: Charge generation and charge transport." *J Lumin* 70 (1996): 48-59.
18. Liu, Xiao-Xia, Ling Zhang, Ya-Bing Li and Li-Jun Bian, et al. "Electrosynthesis of polyaniline/SiO_2 composite at high pH in the absence of extra supporting electrolyte." *Polym Bull* 57 (2006): 825-832.

How to cite this article: Bhaiswar, JB, DP Meghe and SP Dongre. "Study of Thermal Parameter of Polyaniline-Pbs Nanocomposite Using DTA Technique." *J Material Sci Eng* 12 (2023):624.